Liquefaction potential analysis in Yogyakarta – Bawen Toll Road section 3

Shine Farroh Purba[1,2], *Sito* Ismanti[1*], and *Angga Fajar* Setiawan[1]

[1]Department of Civil and Environmental Engineering, Faculty of Engineering, Universitas Gadjah Mada, Yogyakarta, Indonesia
[2]Directorate General of Highways, Ministry of Public Works and Housing, Jakarta, Indonesia

Abstract. The Yogyakarta – Bawen Toll Road construction is one of the National Strategic Projects because it passes through four regencies in Central Java Province and the Special District of Yogyakarta. As the general consideration for infrastructure planning, it was required to consider preventing damages due to natural disasters, including liquefaction caused by an earthquake. The study area has a shallow groundwater table (<10 m), and earthquakes often occurred. Geological conditions showed that the lithologies in Yogyakarta – Bawen Toll Road Section 3 is dominated by silty sand, sandy silt, and gravel. This study aimed to analyze the liquefaction potential in the construction of Yogyakarta – Bawen Toll Road Section 3, especially STA 44+600 – 52+800. The potential liquefaction analysis is calculated using the Simplified Procedure Method based on Standard Penetration Test data. Furthermore, Liquefaction Potential Index (LPI) is applied to determine the level of liquefaction potential. The most central part of the study area indicated no liquefaction potential. On the contrary, the northern and southern parts are indicated to have liquefaction potentials ranging from high to very high. According to the analysis results, it is recommended to have a mitigation plan against liquefaction in the area study.

1 Introduction

Indonesia lies in a zone of intense tectonic activity. It is due to Indonesia's location at the intersection of complex tectonic plate routes formed by the world's three major tectonic plates and several smaller plates [1]. Indonesia is a highly earthquake-prone region due to interactions between these plates. More than 14,000 earthquakes with a magnitude greater than 5.0 Mw were recorded between 1897 and 2009 [2], illustrating the significant seismic activity. A liquefaction catastrophe might be the subsequent effect of an earthquake.

The Yogyakarta - Bawen Toll Road Project is a National Strategic Project because it passes through four Regencies in Central Java and the Special District of Yogyakarta Province. Three districts in Central Java, namely Temanggung Regency, Magelang Regency, and Semarang Regency, while one Regency in the Special Region of Yogyakarta, namely Sleman Regency. The construction of the Yogyakarta - Bawen Toll Road is expected to increase Indonesia's connectivity and economy, particularly in Semarang, Solo, and Yogyakarta, hence supporting the Borobudur Temple Super Priority Tourism Strategic Area. The Yogyakarta - Bawen Toll Road project is susceptible to liquefaction natural disasters because it's close to the subduction zone between the Indo-Australian Plate and the Eurasian Plate and other minor faults. As plate tectonic movements continue, plates can come into collision with these active faults, with the possibility of leading to earthquakes.

The construction of the Yogyakarta - Bawen Toll Road is close to several faults, such as the Merapi and Opak Faults. The Opak Fault is approximately 35-40 km. The Opak Fault became a concern after the Yogyakarta earthquake in May, 2006 because it triggered liquefaction. Numerous liquefaction potential analysis have been conducted due to this large earthquake. Preliminary analysis can be carried out by analyzing geological conditions, grain size analysis, and calculation of safey factor using simplified procedure by Idriss & Boulanger [3].

Study of liquefaction potential has previously been carried out in Yogyakarta – Bawen Toll Road, but only in section I and II. This study concerns to analyze liquefaction potential and susceptibility based on LSI and LPI methods with PGA of 0.322 g and 0.298 g [4]. However, the liquefaction potential analysis in Yogyakarta – Bawen Toll Road Section 3 has not been the focus of any kind of study. According to Atlas of Liquefaction Vulnerability Zones of Central Java and Yogyakarta Provinces, this toll road is included in the moderate liquefaction vulnerability zone [5]. Therefore, it is necessary to conduct study in this location.

The location of this research is focused on the Yogyakarta – Bawen Toll Road Section 3, with a length of 8.1 km, starting from the Borobudur Interchange STA 52+800 to the Magelang Interchange STA 44+600. Fig. 1 shows the construction route plan for the Yogyakarta – Bawen Toll Road Section 3.

*Corresponding author: sito.ismanti@ugm.ac.id

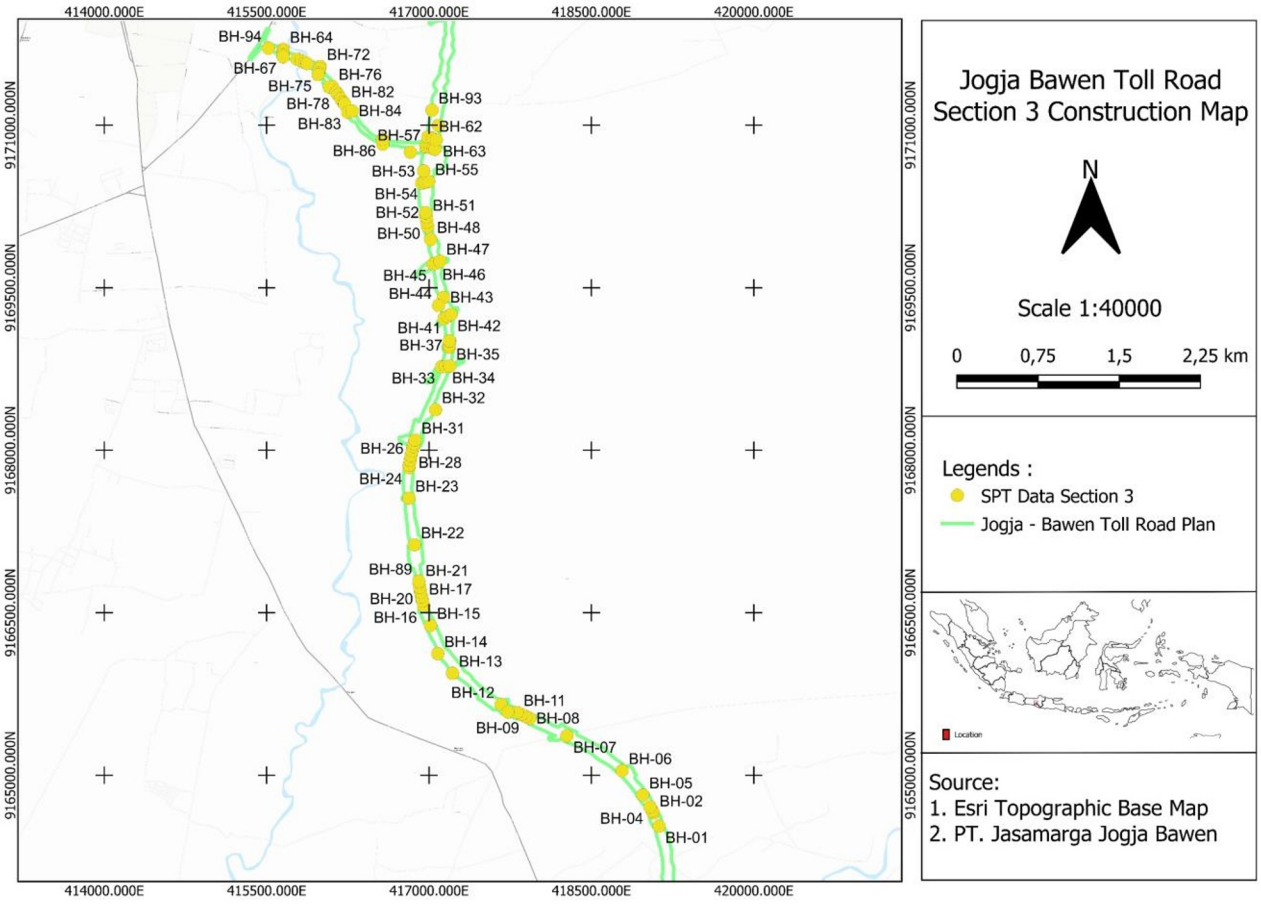

Fig. 1. The construction location of Yogyakarta – Bawen Toll Road Section 3.

This study aims to analyze the liquefaction potential in the Yogyakarta – Bawen Toll Road Section 3 using historical seismic data that has occurred. Analysis of liquefaction potential uses the simplified procedure method by Idriss & Boulanger [6] to determine the safety factor and the liquefaction potential index (LPI) using Sonmez [7].

2 Methodology

2.1 Research data

The data used in this study are soil investigation data (including drilling and standard penetration test data/SPT) and laboratory testing. Field test data was carried out by PT Jasamarga Jogja – Bawen in 2021. Some field test data were carried out in 2 sub-districts in Central Java Province. There are the Mungkid sub-district in the south area and the Candimulyo sub-district in the north area. The total number of SPT data is 94, with 19 SPT drilling data located in the Mungkid sub-district and 75 data in the Candimulyo sub-district. Fig. 2 shows the location of the soil investigation.

2.2 Geological condition

One of the approaches for identifying liquefaction vulnerability is to identify the geological conditions [8]. The construction of Yogyakarta – Bawen Toll Road Section 3 is located in two Regional Geological Map, namely the Magelang Semarang Sheet and the Yogyakarta sheet (Fig. 3).

Fig. 2. Location of the soil investigation.

Based on the regional geological map, there are two rock formations in the construction area of the Yogyakarta – Bawen toll road Section 3, namely the Quarternary-aged Merbabu Volcano Formation and the Quarternary-aged Young Merapi Volcano Deposit Formation. The Quarternary Merbabu Volcano deposits are composed of volcanic breccias and lava, while the Quarternary Merapi Volcano deposits are composed of tuff, ash, breccias, agglomerates, and lava. These loose volcanic deposits result from volcanic eruptions and are susceptible to liquefaction [10].

2.3 Peak ground acceleration determination

The determination of Peak Ground Acceleration (PGA) is carried out using the Probabilistic seismic hazard analysis (PSHA) method through the LINI Binamarga

web-based application [11] developed by the Directorate General of Highways. This application is used to get peak ground acceleration (PGA) values in bedrock with a 7% probability of being exceeded in 75 years of the return period. PGA is determined by entering the locations' coordinates to be reviewed and then obtaining the bedrock PGA. Referring to SNI 1726:2019, the PGA of the bedrock must be multiplied by the site coefficient (FPGA) to get the peak ground acceleration on the surface. [12]. The site coefficient is determined based on the site class classification by calculating the average NSPT value at each borehole.

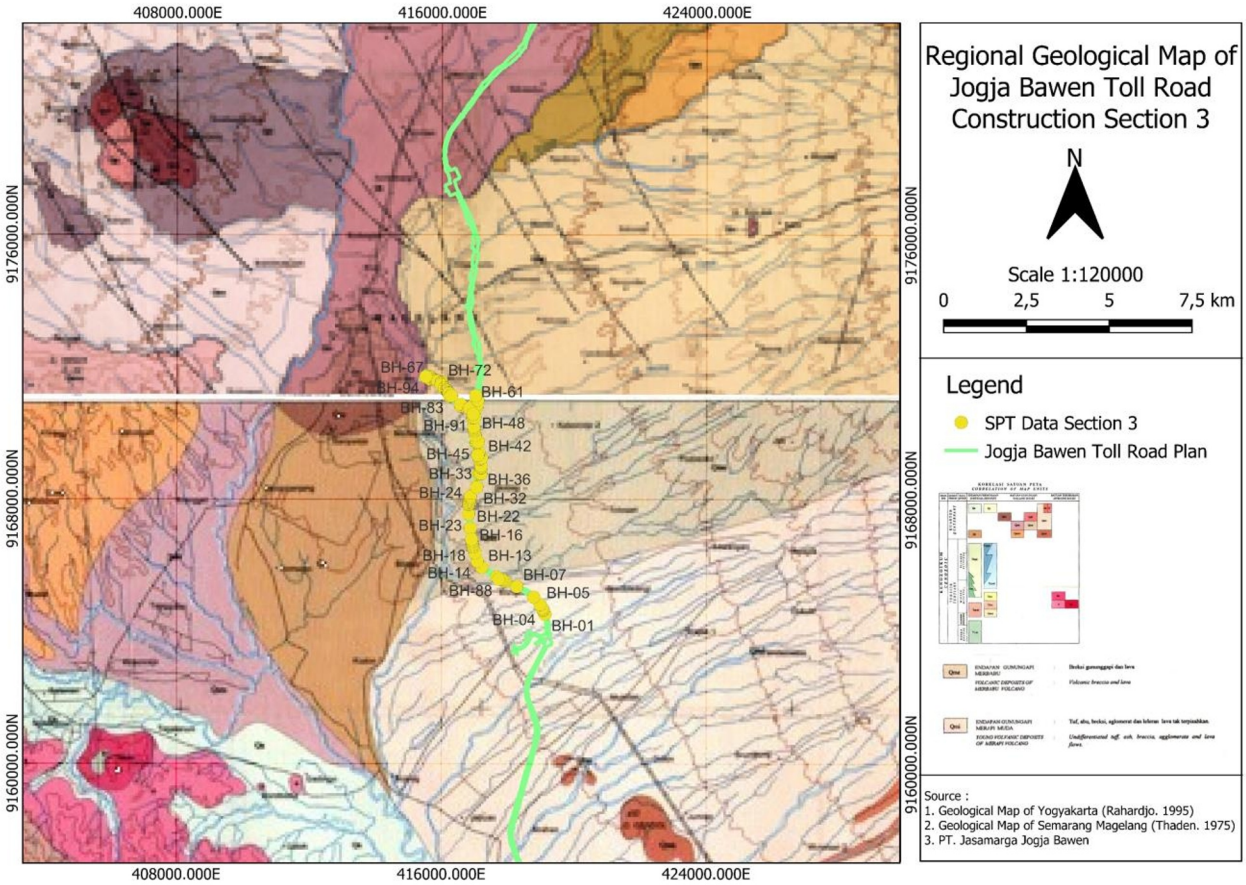

Fig. 3. Regional geological maps of Yogyakarta – Bawen Toll Road section 3 (modified from [9]).

Determination of peak ground acceleration was also carried out using the Deterministic seismic hazard analysis (DSHA) method through the Kanno Attenuation method [13] with the largest earthquake magnitude that ever occurred in the Yogyakarta and Central Java areas, namely 6.3 Mw. This 6.3 MW earthquake originates from the Opak Fault [14]. Based on data from the United States Geological Survey (USGS), several histories of seismicity have occurred with magnitudes above 5 Mw, as shown in Table 1 [15].

Table 1. Earthquake history in research location [15].

No	Year	Lat	Long	Depth (km)	Mw
1	2006	-7.961	110.446	12.5	6.3
2	2001	-7.869	110.179	143.1	6.3
3	1992	-8.474	111.1	63.9	6.1
4	2004	-8.291	109.794	79.9	5.2
5	1979	-7.672	110.755	180	5.2
6	1985	-8.503	110.306	58.9	5.7

Kanno's [13] attenuation method is calculated using Equations 1-2.

$$\log pre = a_1 M_w + b_1 X - \log(X + d_1 10^{0,5M_w}) + c_1 + \varepsilon_1 \quad (1)$$

$$\log pre = a_2 M_w + b_2 X - \log(X) + c_2 + \varepsilon_2 \quad (2)$$

where pre is PGA (cm/sec2), D is earthquake depth (km), a_1, b_1, c_1, d_1, dan ε_1 are regression coefficients for depths less than or equal to 30 km, while a_2, b_1, c_2, d_2, dan ε_2 for depths greater than 30 km. The regression coefficient values are shown in Table 2.

Table 2. Regression coefisien of PGA period.

Event Model	a	b	c	d	ε
Shallow	0.56	-0.0031	0.26	0.0055	0.37
Deep	0.41	-0.0039	1.56	-	0.40

2.4 Liquefaction potential analysis

The liquefaction potential is analyzed using the simplified procedure method by Idriss & Boulanger [6]. The calculation is done by comparing the value of the *Cyclic* Resistance *Ratio* (CRR) with the value of the *Cyclic Stress Ratio* (CSR) in order to obtain the safety factor (FS) for liquefaction. If the SF value < 1, then it is concluded that there is a liquefaction potential.

2.4.1 Cyclic resistance ratio (CRR)

The CRR value indicates the ratio of soil resistance to cyclic loads obtained based on the corrected N-SPT value. The CRR value can increase as the fine content of the soil increases from the corrected N-SPT value.

The N-SPT value is corrected using Equations 3-5, and the CRR value is calculated using Equation 6.

$$(N)_{60} = N_m C_N C_E C_B C_R C_S \quad (3)$$

$$(N_1)_{60cs} = (N_1)_{60} + \Delta(N_1)_{60} \quad (4)$$

$$\Delta(N_1)_{60} = \exp 1.63 + \frac{9.7}{FC + 0.01} - \left(\frac{15.7}{FC + 0.01}\right)^2 \quad (5)$$

$$CRR_{M=7,5,\sigma'_{vc}=1} = \exp\left\{\frac{(N_1)_{60cs}}{14.1} + \left(\frac{(N_1)_{60cs}}{126}\right)^2 - \left(\frac{(N_1)_{60cs}}{23.6}\right)^3 + \left(\frac{(N_1)_{60cs}}{25.4}\right)^4 - 2.8\right\} \quad (6)$$

where, Nm= field test N-SPT value, C_N = overburden correction factor, C_E = energy ratio correction factor, C_B = borehole diameter correction factor, C_R = rod length correction factor, dan C_S = sampling correction factor. The CRR value from equation (6) above is the CRR value with a moment magnitude (Mw) = 7.5 and overburden pressure (σ'vc) = 1 atm. The fines content value is FC <50% based on the Unified Soil Classification System (USCS).

2.4.2 Cyclic stress ratio (CSR)

The CSR value is the shear stress during an earthquake which can trigger liquefaction. CSR value can be calculated using Equation 7.

$$CSR = 0.65 \frac{a_{max}}{g} \frac{\sigma_v}{\sigma'_v} r_d \quad (7)$$

where, a_{max} is the peak ground acceleration on the ground surface, g is the gravity acceleration, σ_v is the total vertical stress, σ'_v is the effective vertical stress, dan r_d is stress reduction factor.

2.5 Liquefaction potential index (LPI)

The liquefaction potential index (LPI) integrates liquefaction potential based on the depth of the soil profile. It predicts the entire performance of the soil column down to one soil layer at a certain depth and depends on the magnitude of the horizontal peaks of soil acceleration [16]. LPI combines depth, thickness, and factor of safety (FS) on liquefaction and predicts the potential for liquefaction resulting in damage to the surface of the observed location.

Iwasaki et al. [17] identified the LPI by assessing earthquake events in Japan from 1975 to 1981. In 2003, Sonmez modified the equation by considering the uncertainty parameter in the liquefaction potential index (LPI) equation and tested liquefaction cases in Inegol City, Turkey. Equations 8-13 sets the safety factor against liquefaction to be 1.2 (F_L) and categorizes the liquefaction level into five categories (Table 3).

$$LPI = \int_0^{20} F(z).w(z).dz \quad (8)$$

$$F(z) = 1 - FL \; for \; FL < 0.95 \quad (9)$$

$$F(z) = 2x10^6 e^{-18.427Fl} \; for \; 0.95 < FL < 1.2 \quad (10)$$

$$F(z) = 0 \; for \; FL \geq 1.2 \quad (11)$$

$$w(z) = 10 - 0{,}5z \; for \; z \geq 20 \; m \quad (12)$$

$$w(z) = 0 \; for \; z \geq 20 \; m \quad (13)$$

Table 3. LPI category based on Sonmez [7].

LPI	Liquefaction Potential
0	No liq
0 < LPI ≤ 2	Low
2 < LPI ≤ 5	Moderat
5 < LPI ≤ 15	High
LPI > 15	Very High

3 Results dan discussion

A geotechnical investigation was conducted to describe the engineering properties of the subsurface soil layer and its relation to the liquefaction potential hazard. In the Yogyakarta – Bawen Toll Road Section 3, there are 94 borehole data. The data show that soil lithologies are dominated by silty sand, sandy silt, and gravel in the south area, whereas sandy clay dominates in the north area. The groundwater table in the study area varies from a minimum depth of 0.5 m to a maximum depth of 20.4 m (Fig. 4). This is due to the morphological conditions in the research area. With a height of 339 m, the morphological characteristics in the beginning area seem relatively flat. Meanwhile towards the end of research area, the morphological conditions are undulating hills with a height of 362 m.

The liquefaction potential was analyzed using the historical magnitude of the largest earthquake in Yogyakarta, 6.3 Mw. The determination of PGA using the probabilistic method through the Lini Binamarga application is summarized in Table 4.

The determination of PGA using a deterministic method is calculated based on Kanno's Attenuation [13] and is summarized in Table 5.Based on the calculations of these two methods, it was found that the most considerable PGA value using the PSHA method from the Lini Binamarga application was 0.35-0.47 while using the DSHA method from Kanno Attenuation [13] was 0.141-0.176 g. This study focuses on bore holes in bold text, since only 4 bore holes have the potential liquefaction at the time of data analysis. The bore holes are BH-07, BH-08, BH-83, and BH-84.

3.1 Grain size distribution analysis

Sandy to silty soils is susceptible to liquefaction. Tsuchida explained that the diversity and grain size of the soil layer affects a soil layer's susceptibility to liquefaction. Fine sandy soils with a grain size of 0.1 – 1 mm and grain size uniformity are generally more susceptible to liquefaction [18]. The grain size distribution plotting can be used for preliminary

liquefaction potential analysis. Based on the grain size distribution of soil, Tsuchida proposes the distribution boundaries of soils prone to liquefaction and potential boundaries to liquefaction. Based on Tsuchida's graph plotting results, four boreholes have the potential for liquefaction, namely at BH-07, BH-08, BH-83, and BH-84 (Fig. 5-8). These four boreholes contain non-cohesive soil samples of sandy soil with uniform gradations. Other boreholes are not analyzed because there are no grain size analysis sample testing data, and some of the data is dominated by clay lithology.

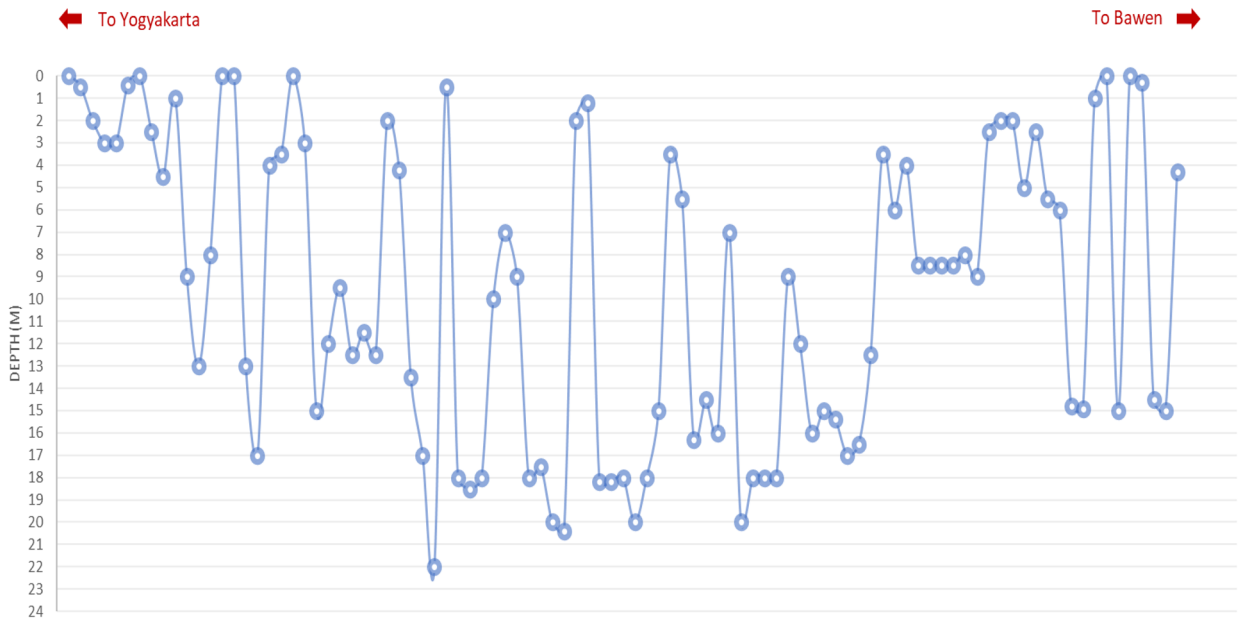

Fig. 4. Profile of groundwater level in the research area.

Table 4. PGA recapitulation using Lini Binamarga.

No	Bore Id	Site Class	PGA	FPGA	PGAM
1	BH-01	SD	0.28	1.32	0.37
2	BH-02	SC	0.28	1.20	0.34
3	BH-03	SC	0.28	1.20	0.34
4	BH-04	SD	0.28	1.32	0.37
5	BH-05	SC	0.28	1.20	0.34
6	BH-06	SD	0.28	1.32	0.37
7	BH-07	SD	0.28	1.32	0.37
8	BH-08	SD	0.28	1.32	0.37
9	BH-09	SC	0.28	1.20	0.34
10	BH-10	SD	0.28	1.32	0.37
11	BH-11	SE	0.28	1.66	0.47
12	BH-12	SE	0.28	1.66	0.47
13	BH-13	SD	0.28	1.32	0.37
14	BH-14	SE	0.28	1.66	0.47
15	BH-15	SE	0.28	1.66	0.47
16	BH-16	SE	0.28	1.66	0.47
17	BH-17	SD	0.28	1.32	0.37
18	BH-18	SD	0.28	1.32	0.37
19	BH-19	SD	0.28	1.32	0.37
20	BH-20	SD	0.28	1.32	0.37
21	BH-21	SE	0.28	1.66	0.47
22	BH-22	SE	0.28	1.66	0.47
23	BH-23	SE	0.28	1.32	0.37
24	BH-24	SE	0.28	1.32	0.37
25	BH-25	SD	0.28	1.32	0.37
26	BH-26	SD	0.28	1.32	0.37
27	BH-27	SD	0.28	1.66	0.47
28	BH-28	SC	0.28	1.20	0.34
29	BH-29	SD	0.28	1.32	0.37

Table 4 (continued). PGA recapitulation using Lini Binamarga.

No	Bore Id	Site Class	PGA	FPGA	PGAM
30	BH-30	SE	0.28	1.66	0.47
31	BH-31	SD	0.28	1.32	0.37
32	BH-32	SD	0.28	1.32	0.37
33	BH-33	SE	0.27	1.69	0.46
34	BH-34	SE	0.27	1.69	0.46
35	BH-35	SD	0.27	1.33	0.36
36	BH-36	SD	0.27	1.33	0.36
37	BH-37	SD	0.27	1.33	0.36
38	BH-38	SD	0.27	1.33	0.36
39	BH-39	SE	0.27	1.69	0.46
40	BH-40	SE	0.27	1.69	0.46
41	BH-41	SE	0.27	1.69	0.46
42	BH-42	SE	0.27	1.69	0.46
43	BH-43	SD	0.27	1.33	0.36
44	BH-44	SC	0.27	1.20	0.32
45	BH-45	SE	0.27	1.69	0.46
46	BH-46	SE	0.27	1.69	0.46
47	BH-47	SE	0.27	1.69	0.46
48	BH-48	SE	0.27	1.69	0.46
49	BH-49	SE	0.27	1.69	0.46
50	BH-50	SD	0.27	1.33	0.36
51	BH-51	SD	0.27	1.33	0.36
52	BH-52	SD	0.27	1.33	0.36
53	BH-53	SE	0.27	1.69	0.46
54	BH-54	SE	0.27	1.69	0.46
55	BH-55	SE	0.27	1.69	0.46
56	BH-56	SD	0.27	1.33	0.36
57	BH-57	SE	0.27	1.69	0.46

Table 4 (continued). PGA recapitulation using Lini Binamarga.

No	Bore Id	Site Class	PGA	FPGA	PGAM
58	BH-58	SE	0.27	1.69	0.46
59	BH-59	SE	0.27	1.69	0.46
60	BH-60	SE	0.27	1.69	0.46
61	BH-61	SE	0.27	1.69	0.46
62	BH-62	SE	0.27	1.69	0.46
63	BH-63	SE	0.27	1.69	0.46
64	BH-64	SE	0.26	1.71	0.45
65	BH-65	SD	0.26	1.34	0.35
66	BH-66	SD	0.26	1.34	0.35
67	BH-67	SE	0.26	1.71	0.45
68	BH-68	SE	0.26	1.71	0.45
69	BH-69	SD	0.26	1.34	0.35
70	BH-70	SD	0.26	1.34	0.35
71	BH-71	SD	0.26	1.34	0.35
72	BH-72	SD	0.26	1.34	0.35
73	BH-73	SD	0.26	1.34	0.35
74	BH-74	SE	0.26	1.71	0.45
75	BH-75	SE	0.26	1.71	0.45
76	BH-76	SE	0.26	1.71	0.45
77	BH-77	SE	0.26	1.71	0.45
78	BH-78	SD	0.27	1.33	0.36
79	BH-79	SD	0.27	1.33	0.36
80	BH-80	SD	0.27	1.33	0.36
81	BH-81	SD	0.27	1.33	0.36
82	BH-82	SE	0.27	1.69	0.46
83	BH-83	SE	0.27	1.69	0.46
84	BH-84	SE	0.27	1.69	0.46
85	BH-85	SE	0.27	1.69	0.46
86	BH-86	SE	0.27	1.69	0.46
87	BH-87	SE	0.27	1.69	0.46
88	BH-88	SE	0.27	1.69	0.46
89	BH-89	SE	0.27	1.69	0.46
90	BH-90	SD	0.27	1.33	0.36
91	BH-91	SD	0.27	1.33	0.36
92	BH-92	SE	0.27	1.69	0.46
93	BH-93	SE	0.27	1.69	0.46
94	BH-94	SD	0.26	1.34	0.35

Table 5. PGA recapitulation using Kanno's attenuation.

No	Bore Id	Epicenter (km)	Hipocenter (km)	Log PGA	PGA (g)
1	BH-01	48.78	50.36	2.238	0.176
2	BH-02	48.91	50.48	2.236	0.176
3	BH-03	48.94	50.51	2.236	0.176
4	BH-04	48.99	50.56	2.235	0.175
5	BH-05	49.11	50.67	2.234	0.175
6	BH-06	49.39	50.95	2.231	0.174
7	BH-07	49.89	51.43	2.226	0.172
8	BH-08	50.18	51.71	2.223	0.170
9	BH-09	50.22	51.76	2.223	0.170
10	BH-10	50.27	51.80	2.222	0.170
11	BH 11	50.31	51.84	2.222	0.170
12	BH 12	50.37	51.90	2.221	0.170
13	BH 13	50.45	51.98	2.221	0.169
14	BH 14	51.09	52.59	2.214	0.167
15	BH 15	51.38	52.88	2.211	0.166
16	BH 16	51.55	53.04	2.210	0.165

Table 5 (continued). PGA recapitulation using Kanno's attenuation.

No	Bore Id	Epicenter (km)	Hipocenter (km)	Log PGA	PGA (g)
17	BH 17	51.59	53.08	2.209	0.165
18	BH 18	51.65	53.14	2.209	0.165
19	BH 19	51.67	53.16	2.208	0.165
20	BH 20	51.72	53.21	2.208	0.165
21	BH 21	51.76	53.25	2.207	0.164
22	BH 22	52.08	53.56	2.204	0.163
23	BH 23	52.51	53.98	2.200	0.162
24	BH 24	52.79	54.25	2.197	0.161
25	BH-25	53.11	54.56	2.194	0.159
26	BH-26	53.46	54.9	2.191	0.158
27	BH-27	53.86	55.29	2.187	0.157
28	BH-28	54.30	55.72	2.183	0.155
29	BH-29	54.78	56.19	2.178	0.154
30	BH-30	55.29	56.68	2.173	0.152
31	BH-31	55.83	57.21	2.168	0.150
32	BH-32	56.71	58.07	2.159	0.147
33	BH-33	56.75	58.11	2.159	0.147
34	BH-34	56.76	58.12	2.159	0.147
35	BH-35	56.76	58.12	2.159	0.147
36	BH-36	56.94	58.29	2.157	0.146
37	BH-37	56.96	58.32	2.157	0.146
38	BH-38	56.99	58.35	2.157	0.146
39	BH-39	57.00	58.35	2.157	0.146
40	BH-40	57.21	58.56	2.155	0.146
41	BH-41	57.22	58.57	2.155	0.146
42	BH-42	57.24	58.59	2.154	0.145
43	BH-43	57.35	58.70	2.153	0.145
44	BH-44	57.40	58.75	2.153	0.145
45	BH-45	57.74	59.07	2.150	0.144
46	BH-46	57.74	59.07	2.150	0.144
47	BH-47	57.69	59.02	2.150	0.144
48	BH-48	57.96	59.29	2.148	0.143
49	BH-49	58.09	59.41	2.147	0.143
50	BH-50	58.13	59.45	2.146	0.143
51	BH-51	58.17	59.50	2.146	0.143
52	BH-52	58.21	59.54	2.145	0.142
53	BH-53	58.49	59.81	2.143	0.142
54	BH-54	58.49	59.81	2.143	0.142
55	BH-55	58.51	59.83	2.143	0.142
56	BH-56	58.55	59.87	2.142	0.141
57	BH-57	58.82	60.14	2.140	0.141
58	BH-58	58.82	60.14	2.140	0.141
59	BH-59	58.81	60.13	2.140	0.141
60	BH-60	58.81	60.12	2.140	0.141
61	BH-61	55.47	56.86	2.171	0.151
62	BH-62	55.43	56.82	2.172	0.151
63	BH-63	55.41	56.80	2.172	0.151
64	BH-64	57.54	58.88	2.152	0.145
65	BH-65	57.26	58.61	2.154	0.145
66	BH-66	56.88	58.24	2.158	0.147
67	BH-67	56.61	57.97	2.160	0.147
68	BH-68	56.61	57.98	2.160	0.147
69	BH-69	56.59	57.95	2.161	0.148
70	BH-70	56.57	57.93	2.161	0.148
71	BH-71	56.54	57.90	2.161	0.148
72	BH-72	56.47	57.83	2.162	0.148
73	BH-73	56.42	57.79	2.162	0.148

Table 5 (continued). PGA recapitulation using Kanno's attenuation.

No	Bore Id	Epicenter (km)	Hipocenter (km)	Log PGA	PGA (g)
74	BH-74	56.39	57.76	2.163	0.148
75	BH-75	56.37	57.74	2.163	0.148
76	BH-76	56.25	57.62	2.164	0.149
77	BH-77	56.26	57.63	2.164	0.149
78	BH-78	55.95	57.33	2.167	0.150
79	BH-79	55.71	57.10	2.169	0.150
80	BH-80	55.45	56.84	2.171	0.151
81	BH-81	55.31	56.70	2.173	0.152
82	BH-82	55.26	56.66	2.173	0.152
83	BH-83	55.97	57.35	2.166	0.150
84	BH-84	55.97	57.35	2.167	0.150

Table 5 (continued). PGA recapitulation using Kanno's attenuation.

No	Bore Id	Epicenter (km)	Hipocenter (km)	Log PGA	PGA (g)
85	BH-85	55.52	56.91	2.171	0.151
86	BH-86	55.62	57.00	2.170	0.151
87	BH-87	55.40	56.79	2.172	0.151
88	BH-88	50.32	51.85	2.222	0.170
89	BH-89	51.77	53.26	2.207	0.164
90	BH-90	51.78	53.27	2.207	0.164
91	BH-91	58.61	59.93	2.142	0.141
92	BH-92	55.53	56.92	2.171	0.151
93	BH-93	55.68	57.07	2.169	0.151
94	BH-94	56.81	58.17	2.159	0.147

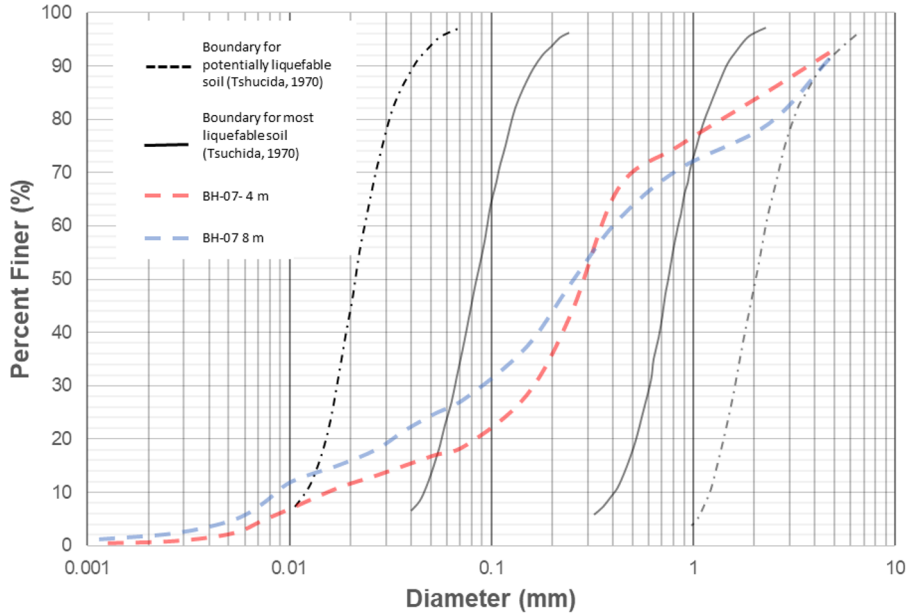

Fig. 5. Grain size analysis for BH-07.

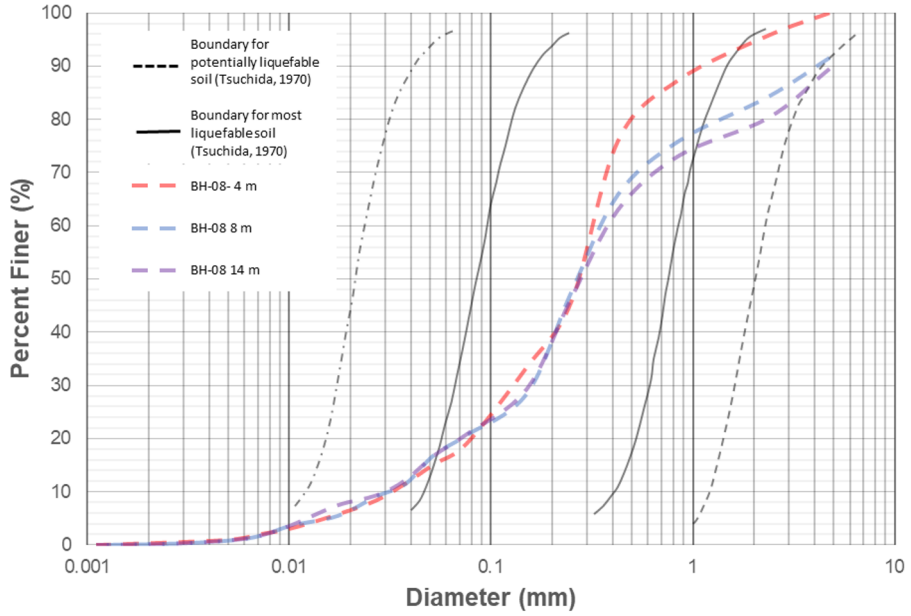

Fig. 6. Grain size analysis for BH-08.

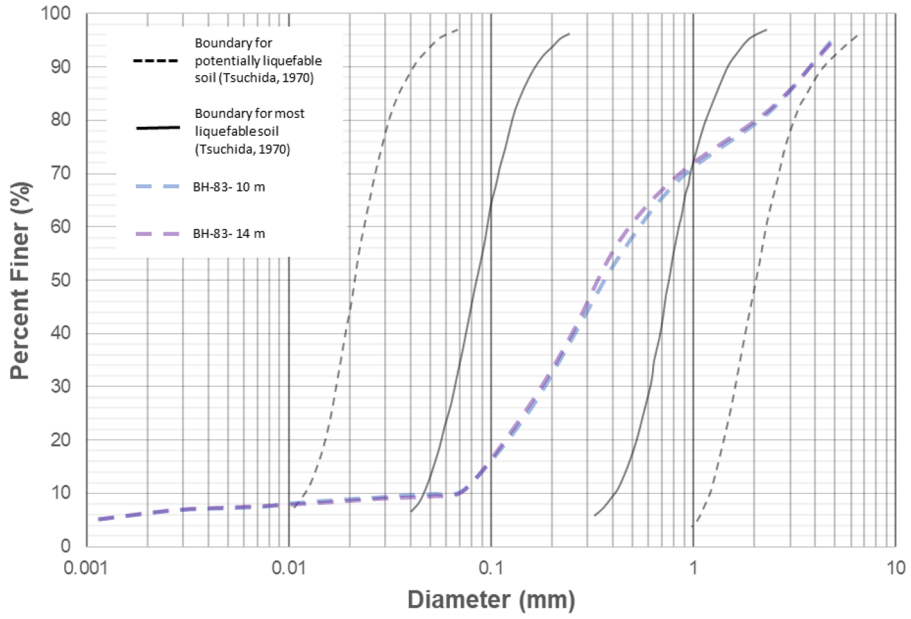

Fig. 7. Grain size analysis for BH-83.

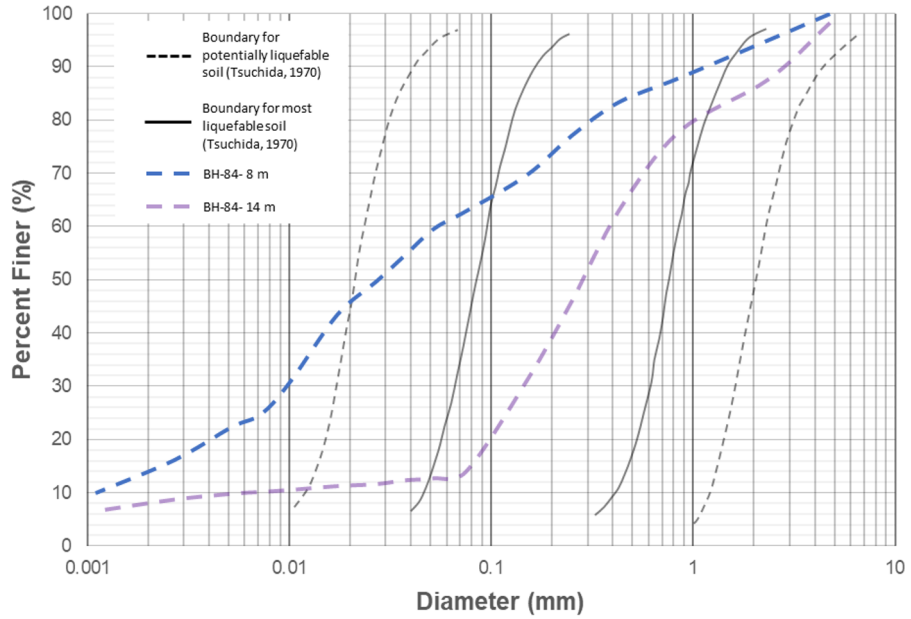

Fig. 8. Grain size analysis for BH-84.

3.2 Safety factor

Based on the results of liquefaction potential analysis calculations using the Idriss & Boulanger [6] method, there are four boreholes, namely BH-07, BH-08, BH-83, and BH-84 which have FS value < 1 and are found in several layers of soil depth. At BH-07, the liquefaction potential soil layer is at 8 m and 12 m. At BH-08, the soil layer with the liquefaction potential is at a depth of 12 - 14 m. At BH-83, the soil layer with the liquefaction potential is at a depth of 8 – 14 m. At BH-84, the soil layer with the liquefaction potential is at a depth of 10 – 14 m. Soil layers with FS value < 1 are dominated by a layer of soil in the form of sand with saturated conditions, relatively uniform grain sizes, and contained by an NSPT value < 20. Fig. 9-10 show the FS values for each borehole BH-07, BH -08, BH-83, and BH-84.

3.3 Liquefaction potential index

Safety factor (FS) influences the liquefaction potential index. If the FS value is smaller, the LPI value will be greater, and vice versa. LPI value is determined using Equation 8, and PGA is determined using two methods: the PSHA method from Lini Binamarga and the DSHA based on Kanno's Attenuation [13]. The magnitude of the earthquake used was 6.3 *Mw*. Table 6 shows the recapitulation of LPI values based on the two methods mentioned above.

The LPI value using the PGA from Lini Binamarga indicates that the liquefaction potential index is in the moderate to very high range, while the LPI value using the PGA from Kanno Attenuation [13] indicates that the liquefaction potential index is in the non-liquefied-to-high-range.

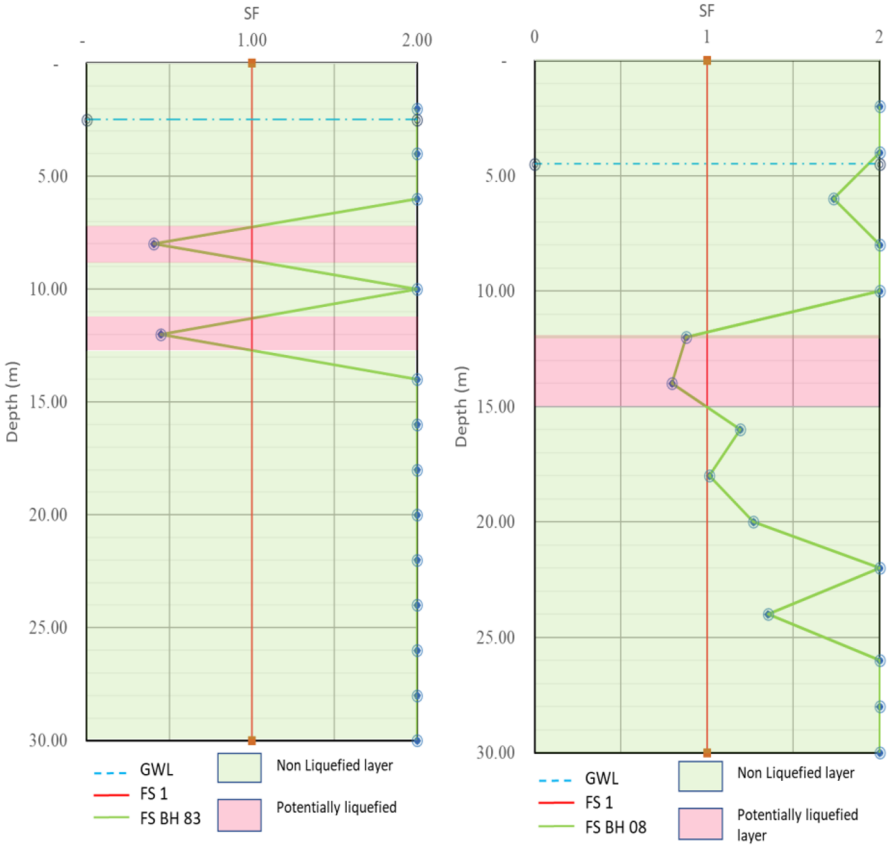

Fig. 9. Safety Factor BH-07 and BH-08.

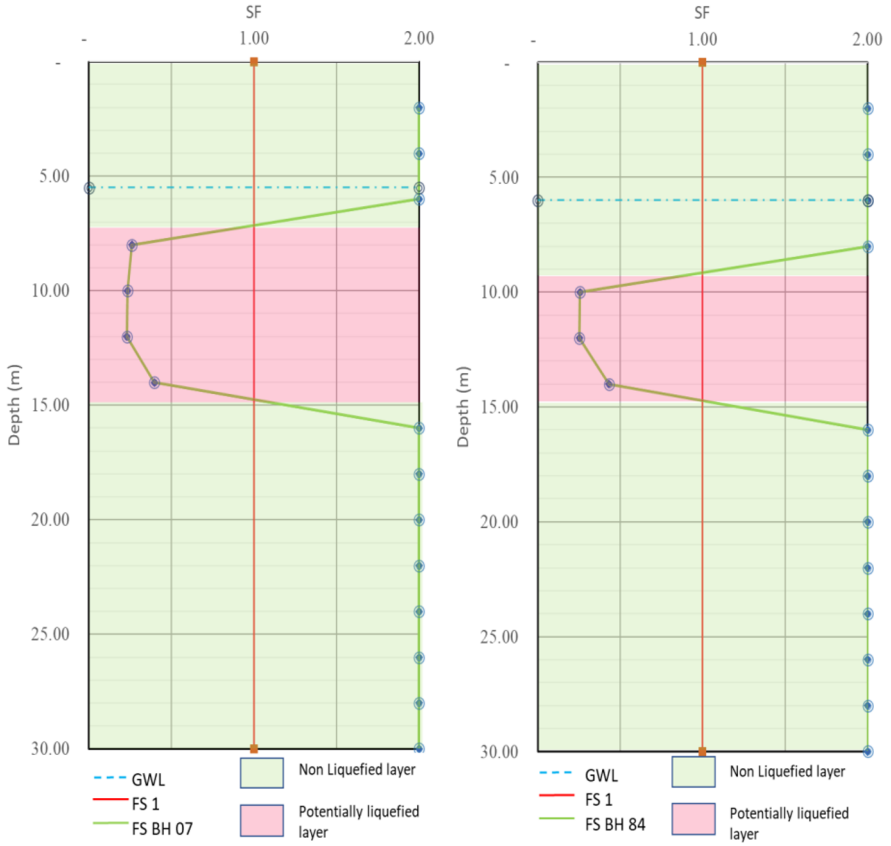

Fig. 10. Safety Factor BH-83 and BH-84.

Table 6. Recapitulation of LPI.

Bore Id	PSHA Lini Binamarga		DSHA Kanno Atenuasi	
	LPI	Category	LPI	Category
BH-07	11.57	High	1.78	Low
BH-08	2.21	Mod	0.00	No Liq
BH-83	26.31	Very High	7.73	High
BH-84	16.82	Very High	4.03	Mod

4 Conclusions

The Yogyakarta – Bawen Toll Road Project Section 3 has liquefaction potential at several locations based on borehole data obtained from PT. Jasa Marga Jogja Bawen. According to soil investigation data, the soil lithology at the research location is dominated by silt sand, sandy silt, and gravel. In several locations, the shallow groundwater level is less than 2 m, but it gets deeper, up to 18 m. It is because the research locations starting from the southern region are relatively plain in morphology and increasingly to the north in undulating hill morphology. It also resulted in the liquefaction potential in the study area not being spread evenly but only in a few locations with shallow groundwater tables, loose silty sand dominant lithology, and NSPT values <20.

Based on the earthquake history that occurred in the Yogyakarta and Central Java areas in 2006, 2 PGA calculation methods are carried out. The first method is based on the PSHA from the Lini Binamarga with a PGA value of 0.35 – 0.47 g. The second method is based on DSHA from the Kanno Attenuation [13] with a PGA value of 0.141 – 0.176 g.

Liquefaction potential analysis was carried out at 94 boreholes spread from south to north, starting from Mungkid District to Candimulyo District, Central Java Province, and using the Liquefaction Potential Index (LPI) method. Based on the analysis using PGA from the Lini Binamarga, liquefaction potential index ranging from moderate to very high were obtained, and PGA based on Attenuation Kanno [13] obtained liquefaction potential index ranging from not liquefied to high.

Based on the potential liquefaction analysis that has been carried out, further research and calculations are needed to plan appropriate and effective mitigation at locations that have a high level of liquefaction potential.

The authors gratefully thank for the support given by Directorate of Freeways, Directorate General of Highway, Ministry of Public Works and Housing.

References

1. P. Bird, Geochemistry, Geophysics, Geosystems **4**(3), 1027 (2003) https://doi.org/0.1029/ 2001GC000252
2. M. Asrurifak, M. Irsyam, B. Budiono, W. Triyoso, H. Hendriyawan, Civil Engineering Dimmension **12**(1), 52-62 (2010) https://doi.org/10.9744/ced.12.1.52-62
3. A. Zakariya, F. Nurdiansyah, C.T.S.A. Galag, J. Situmorang, Jurnal Jalan-Jembatan **39**(2), 74-87 (2022)
4. P. Kevin, M. Muhrozi, Civil Engineering Dimension **25**(1), 29-36 (2023) https://doi.org/10.9744/ced.25.1.29-36
5. T.W. Buana, W. Hermawan, R.N. Rahdiana, R.W. Wahyudin, G. Hasibuan, Wiyono, W.P. Sollu, Atlas of liquefaction vulnerable zone of Indonesia (Geology Agency, Ministry of Energy and Mineral Resources, 2019)
6. R.W. Boulanger, I.M. Idriss, CPT and SPT based liquefaction triggering procedures (Center for Geotechnical Modeling, 2014)
7. H. Sonmez, Env Geol **44**, 862-871 (2003) https://doi.org/10.1007/s00254-003-0831-0
8. S.L. Kramer, Geotechnical earthquake engineering (Prentice-Hall. Inc., 1996)
9. Ministry of Energy and Mineral Resources, Geological maps of Yogyakarta and Semarang Magelang (Accessed 28 Jan 2022) https://geologi.esdm.go.id
10. T.W. Buana, M. Wafid AN, I.A. Sadisun, Jurnal Lingkungan dan Bencana Geologi **7**(2), 103-111 (2016) https://dx.doi.org/10.34126/jlbg.v7i2.98
11. Directorate of Road and Bridge Engineering, Indonesia earthquake source and hazard map for bridges 2017, aplikasi lini (Accessed 28 Jan 2022) https://lini.binamarga.pu.go.id/
12. National Standardization Agency, Earthquake resistance planning procedures for building and non-building structures (SNI 1726:2019)
13. T. Kanno, A. Narita, N. Morikawa, H. Fujiwara, Y. Fukushima, Bulletin of the Seismological Society of America **96**(3), 879-897 (2006) https://doi.org/10.1785/0120050138
14. A. Sutiono, B. Pratistho, C. Prasetyadi, Supartoyono, IOP Conf. Ser.: Earth Environ. Sci. **212**, 012049 (2018) DOI 10.1088/1755-1315/212/1/012049
15. United States Geological Survey, Earthquake history in research location (Accessed 30 Jan 2022) https://earthquake/usgs.gov/earthquakes/ map
16. R. Luna, J.D. Frost, Journal of Computing in Civil Engineering **12**(11), 48-56 (1998) https://doi.org/10.1061/(ASCE)0887-3801(1998)12:1(48)
17. T. Iwasaki, K. Tokida, F. Tatsuoka, *Soil liquefaction potential evaluation with use of the simplified procedure*, in Proceedings of the International Conferences on Recent Advances in Geotechnical Earthquake Engineering and Soil Dynamics, 26 April-3 May 1981, St Louis, Missouri (1981) https://scholarsmine.mst.edu/icrageesd/01icrageesd/session02/12

18. H. Tsuchida, *Prediction and countermeasure againts liquefaction in sand deposits*, in Proceedings of the 16th LACCEI International Multi-Conference for Engineering, Education, and Technology, 19-21 July 2018, Lima, United States (2018)